Journal of Molecular Catalysis A: Chemical 333 (2010) 121–127

Contents lists available at ScienceDirect

Journal of Molecular Catalysis A: Chemical

journal homepage: www.elsevier.com/locate/molcata

DeNO$_x$ activity–TPD correlations of NH$_3$-SCR catalysts

B. Greenhalgh*, M. Fee, A. Dobri, J. Moir, R. Burich, J.-P. Charland, M. Stanciulescu

CanmetENERGY - Innovation and Energy Technology Sector, Natural Resources Canada, 1 Haanel Drive, Nepean, Ontario K1A 1M1, Canada

ARTICLE INFO

Article history:
Received 3 December 2009
Received in revised form
25 September 2010
Accepted 3 October 2010
Available online 11 November 2010

Keywords:
Zeolite acidity
DeNO$_x$
NH$_3$-SCR
NH$_3$-TPD
Aftertreatment

ABSTRACT

A series of Mn-exchanged zeolite catalysts was tested for its DeNO$_x$ activity in ammonia selective catalytic reduction (NH$_3$-SCR) reactions. Activity was found to depend strongly on metal loading such that at low Mn content, NO$_x$ conversion is limited to 50% at 700 K. However, above a mass percentage of Mn between 1.6 and 1.9%, near complete NO$_x$ conversion is achieved at 525 K. Ammonia – temperature programmed desorption (NH$_3$-TPD) was used in an attempt to explain the findings of these experiments. Specifically, we have used NH$_3$-TPD to determine the population and strength of the acid sites present in the catalysts as a function of Mn content. Acid sites with adsorption energies ranging from 45 to 68.7 kJ/mole have been detected. At temperatures where DeNO$_x$ activity differs significantly among the catalysts, corresponding differences in their acid site distributions, and hence surface NH$_3$ populations, are observed.

Crown Copyright © 2010 Published by Elsevier B.V. All rights reserved.

1. Introduction

The environmental impacts of mononitrogen oxides, collectively termed NO$_x$, are well-known [1]. These effects include the formation of acid rain, particulate matter and photochemical smog, as well as stratospheric ozone depletion and ground level ozone formation. This has motivated stringent environmental legislation on the allowable NO$_x$ content in engine exhaust. An example of this is the 2010 EPA Tier 2 Bin 5 emission standards, which demand that light duty diesel vehicles emit no more than 0.05 g of NO$_x$ per mile [2]. Historically, engine manufacturers have kept pace with such legislation through innovations such as exhaust gas recycling (EGR) and homogeneous charge compression ignition (HCCI) [3,4]. However, in order to continue to meet these standards, aftertreatment technologies for the suppression of NO$_x$ levels in engine exhaust will require significant development [5].

A key aftertreatment technology is the on-stream reduction of NO$_x$ to N$_2$ and H$_2$O using a reductant such as NH$_3$ over a suitable catalyst. This is known as ammonia – selective catalytic reduction (NH$_3$-SCR), and can be represented by general reaction schemes such as:

$$4NO + 4NH_3 + O_2 \rightarrow 4N_2 + 6H_2O \quad (1)$$

$$4NO_2 + 6NH_3 + 1/2O_2 \rightarrow 5N_2 + 9H_2O \quad (2)$$

A primary challenge to be overcome in the development of such catalysts is the wide range of operating temperatures under which these catalysts must perform. For example, in automotive applications, reaction conditions vary significantly. During so-called cold-start conditions (in which the catalyst has not yet reached the optimum operating temperature) unreacted NH$_3$ can pass by the catalyst leading to what is commonly referred to as ammonia slip. At the other extreme, high operating temperatures can lead to a drop in selectivity to N$_2$, with a corresponding production of oxidized byproducts favored by equilibrium, particularly in lean (high O$_2$) applications such as diesel engines. Thus, a successful SCR catalyst must simultaneously maintain high NO$_x$ conversion over the widest possible range of exhaust temperatures.

Metal exchanged zeolites are attracting significant research attention as potential catalysts for SCR reactions [6]. The utility of zeolites as catalyst supports derives significantly from their remarkable ion-exchange capacity [7]. Contacting a suspension of the zeolite with an aqueous solution of metal cations results in cation incorporation within the zeolite framework, and thus allows the introduction of a catalytically active phase. In addition, aluminosilicate zeolites posses an inherent acidity, due to both Brønsted and Lewis sites [7]. For this reason, metal exchanged zeolites find use in applications where both metallic and acidic functions are required. Examples include ring opening and isomerisation [8,9] and hydrotreating [10,11]. In keeping with charge neutrality, the introduction of metal cations by ion-exchange within the framework of the acidic form of a zeolite displaces protons from the structure. In addition, the incorporation of polyvalent ions can result in regions of low electron density, and thus increased Lewis acidity. Recent literature reports have indicated the relationship

* Corresponding author. Tel.: +1 403 250 4751; fax: +1 403 291 0633.
E-mail address: greenhab@novachem.com (B. Greenhalgh).

1381-1169/$ – see front matter. Crown Copyright © 2010 Published by Elsevier B.V. All rights reserved.
doi:10.1016/j.molcata.2010.10.008

between acidity and activity in NH_3-SCR reactions. An example of this is the work of Putluru et al. [12] which demonstrates how activity increases with acidity in vanadia/zeolite SCR catalysts. It is then expected that a series of metal exchanged zeolites would show a variation in both catalytic activity and acidity as the degree of exchange increases.

The objective of the current study was to conduct a systematic comparison of the $DeNO_x$ activity of Mn exchanged zeolites with regard to changes in their acidity. We have therefore attempted to correlate variations in the NH_3-SCR activity of a series of Mn containing zeolites with the observed variations in their NH_3-temperature programmed desorption (TPD) behavior. This is a well-known catalyst characterization technique which is used to determine the acidity of a solid catalyst. By dosing a sample with NH_3, and then raising the temperature in a controlled manner to bring about desorption, a quantitative statement of the strength and population of acid sites present in the sample can be made. Such NH_3-TPD results have been used in order to rationalize the observed trend in activity of Mn-exchanged zeolite catalysts in NH_3-SCR reactions for NO_x reduction. The study finds that low temperature SCR activity increases with Mn loading, until a threshold Mn content between 1.6% and 1.9%, above which activity tends to plateau with further Mn loading. Corresponding increases and plateaus in the density of certain acid sites which retain NH_3 under the same conditions at which high SCR activity are observed, suggesting a correlation between the catalyst acidity and SCR activity.

2. Experimental

2.1. Catalyst preparation

CBV-2314, an NH_4-form of ZSM-5 with molar Si/Al of 11.5 (Zeolyst International), was exchanged with aqueous solutions of $Mn(NO_3)_2$ (Aldrich). Typically, 4 g of CBV-2314 was suspended in 400 mL of deionized water, with varying amounts of $Mn(NO_3)_2$. The suspension was heated to 350 K and stirred for 4 h, before the heating was switched off, and the suspension was stirred overnight. The next morning, the solids were filtered and washed with two 150 mL portions of deionized H_2O, dried at 400 K then calcined at 873 K for 6 h in air. By varying the amount of $Mn(NO_3)_2$ used in the exchange process, and by performing repeat exchanges, a series of catalysts of increasing Mn content, ranging in mass percentage from 0 to 3.2% was produced.

2.2. Catalyst characterization

2.2.1. Sample composition

Sample compositions were determined using a Hitachi S3400N VP-SEM with an Oxford INCA EDX detector system operating at 20 kV and 80 mA. Oxidation state determinations were conducted using a Kratos XPS system operating at 10^{-10} Torr. Binding energies were referenced to the C 1s feature assigned to 285.0 eV.

2.2.2. Surface area

The BET surface areas of the catalysts were measured using a Micromeritics ASAP 2020 instrument by nitrogen adsorption at 77 K. Each sample was degassed for 16 h at 473 K before the isotherms were measured.

2.2.3. Acidity

NH_3-TPD data were collected on a Micromeritics Autochem 2920 II Automated Catalyst Characterization System. Each sample (ca. 150 mg of finely ground powder) was initially pretreated through heating in 50 mL/min of pure He from ambient at 50 K/min to 873 K, with a 2 h hold. Next, the sample temperature was stabilized at T_{Ads} (for example 443 K), after which the sample was dosed with 50 mL/min of 15% NH_3/He for 15 min. Next, the sample was flushed with 50 mL/min of He for 15 min to remove weakly bound (physisorbed) NH_3, after which the sample temperature was reduced to 323 K. Once a stable baseline by TCD (thermal conductivity detector) had been achieved, the temperature was then ramped from 323 K at a rate of 5 K/min to 873 K, at which the temperature was held for 2 h. During this process, the desorption rate was monitored by TCD. The experiments were repeated at varying adsorption temperatures (i.e. T_{Ads} = 443, 463, 483, ...773 K), in order to deconvolute the resulting desorption behaviour into acid sites with distinct energy values. A detailed description of the deconvolution procedure can be found in the work of Costa et al. [13], whereas herein only the essential explanation will be given. The choice of T_{Ads} was varied until the subtraction of desorption data corresponding to sequential T_{Ads} values could be fit to a normalized first order desorption equation, analogous to that given by Costa et al. [13]:

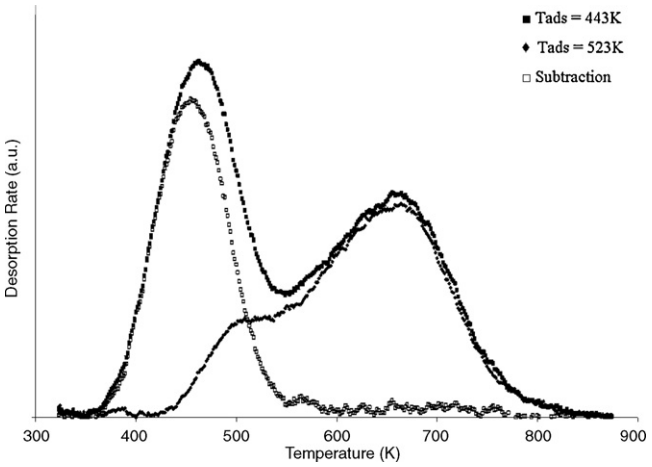

Fig. 1. Subtraction of desorption data to yield acid sites of uniform strength.

$$\frac{q}{q_o} = \exp\left(-\frac{k_E}{\beta}\int_{T_o}^{T}\exp\left(\frac{-E_A}{RT}\right)dT\right) \quad (3)$$

In Eq. (3), q and q_o (moles) are the quantities of ammonia adsorbed on a given acid site at temperatures T and T_o (K), respectively, while β (K/min) is the temperature ramp rate employed in the experiment. The symbols K_E (1/min) and E_A (J/mole) are the exponential pre-factor and activation energy of ammonia desorption from the acid site. R is the universal gas constant with value 8.3145 J/K*mole. Each such subtraction and fit generated two parameters, K_E/β and E_A/R, as shown in Figs. 1 and 2. At a given heating rate β the values of K_E and E_A can easily be calculated. The work of Costa et al. generated a basis of energies (E_A) for use in the deconvolution via the following equation:

$$K_E = \alpha\exp(\beta E) \quad (4)$$

Once the parameters α and β have been determined, an arbitrary set of E_A values can be chosen for which K_E values can be calculated. Preliminary experiments in this study produced values of k_E and E_A which, despite the fact that these parameters were derived from satisfactory data fits, (i.e. they resulted from uniform acidity desorption rate data), and consisted of comparable E_A values as reported by Costa et al. they were not well-represented by Eq. (4). This may be due in part to the fact that the present study is concerned with changes in acidity upon increased metal content. As a result, a set of k_E/β and E_A/R values (determined through direct measurement) was developed in order to deconvolute the desorption data of the MnCBV-2314 series. The set of k_E/β and E_A/R values was expanded until satisfactory deconvolution of samples

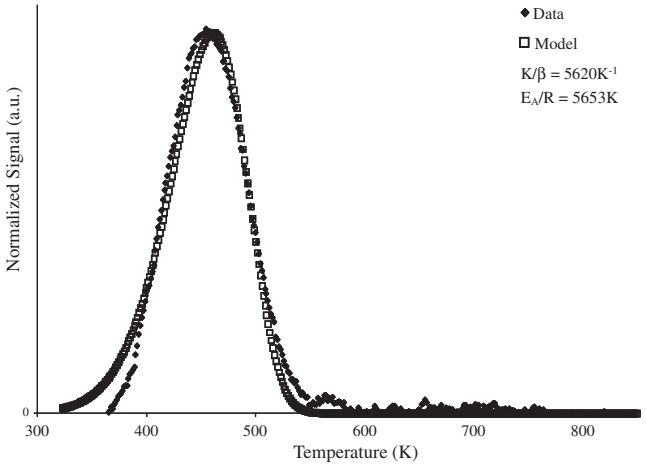

Fig. 2. Fitting of uniform strength acid sites to yield desorption rate parameters.

with both low and high Mn content in our series was achieved. The population of each acid site (q_o value) present in each sample was determined by minimizing the residual between the desorption data (per unit mass of sample) and the model consisting of the parameter values for K_E/β and E_A/R. Finally, this set was considered to be a *basis* for the catalyst series and was thus applied to the samples of intermediate Mn loadings. The relative population of each acid site in each sample was then calculated as a percentage of all sites present. It is important to note that the K_E/β and E_A/R values result from subtractions of two desorption experiments. As a result, before the desorption rate data for a given sample can be deconvoluted, the desorption rate data corresponding to the maximum T_{Ads} value used in the experiments must first be subtracted. This procedure is represented in Fig. 3.

2.2.4. Catalytic activity measurements

The catalysts were tested in a flow reactor system, the details of which are published elsewhere [5]. In the present work, the feed consisted of 500 ppmv NH_3, 500 ppmv NO, 50 000 ppmv O_2 and 50 000 ppmv H_2O in He at a flowrate of 1000 mL/min (GHSV = 80 000 h^{-1}). The temperature was ramped from 350 K to 573 K at 1 K/min, followed by a ramp from 573 K to 723 K at 2 K/min. NO_x concentrations were monitored by a Thermo Environmental model 42H chemiluminescence NO_x analyzer.

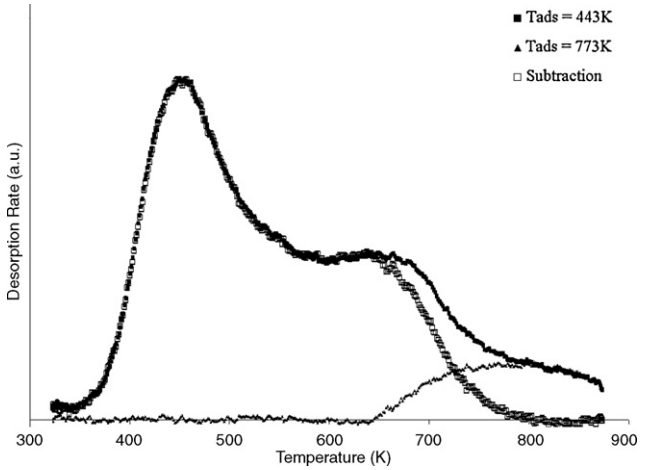

Fig. 3. Subtraction of desorption rate data to allow complete deconvolution.

Table 1
Catalyst compositions by SEM/EDX and surface areas by BET.

Catalyst name	Composition (mass %)				BET surface area (m^2/g)
	Mn	Si	Al	Si/Al (mol/mol)	
CBV-2314	0	43.4	3.6	11.6	352
0.5%MnCBV-2314	0.5	43.2	3.6	11.6	361
1.6%MnCBV-2314	1.6	42.6	3.5	11.7	344
1.9%MnCBV-2314	1.9	42.5	3.5	11.7	360
2.2%MnCBV-2314	2.2	41.9	3.5	11.5	362
2.5%MnCBV-2314	2.5	42.3	3.4	12.0	366
2.8%MnCBV-2314	2.8	41.9	3.6	11.2	345
3.2%MnCBV-2314	3.2	41.7	3.5	11.5	340

3. Results and discussion

3.1. Characterization

3.1.1. SEM/EDS, XPS and surface area

The measured compositions of the catalysts are shown in Table 1. The catalysts were named according to their Mn content as measured by SEM/EDX. The molar Si/Al ratio has also been calculated and listed in Table 1. As there is little variation from the expected value of 11.5, (as rated by the manufacturer), it appears that the ion-exchange has not compromised the structural framework of the zeolite (i.e. no Al leaching has occurred). Limited XPS studies indicate that Mn, characterized by a broad Mn 2p feature centred at 643.0 eV, is present within these catalysts in the following oxidation states: Mn(II), Mn(III) and Mn(IV) [14,15]. Table 1 also lists the BET surface areas of the catalyst in the series. As no significant variation occurs with increasing exchange, this is further evidence that no structural degradation of the support occurred.

3.1.2. NH_3-TPD

The set of parameter values derived from the basis are listed in Table 2, and a typical acid site distribution result is shown in Fig. 4. A total of seven acid sites were identified in the Mn series, with E_A values (equivalent to heats of NH_3 adsorption [16]) ranging from 45.2 to 68.7 kJ/mole. This range is very similar to that reported by Costa et al. in their work on zeolite Y [13] and on ZSM-5 [17] type zeolites. Furthermore, the general shape of the TPD data for these catalysts, in particular the major desorption peaks near 450 K and 650 K, are in agreement with the work of Costa et al. [17] on similar materials under comparable conditions.

3.2. SCR activity testing

The activity of each of the catalysts in the series is shown in Fig. 5. As is clearly seen, CBV-2314 shows poor activity at low temperature, but exhibits significant activity at high temperature, reaching nearly 50% NO_x conversion at 700 K. The favorable effect of Mn

Table 2
Parameter values used in TPD deconvolutions.

ΔT_{Ads}	Parameter values				
	T_P (K)	E_A/R (K)	E_A (kJ/mole)	K_E/β (K^{-1})	K_E (s^{-1})
(443–523 K)[b]	443	5437	45.2	5411	451
(443–523 K)[a]	457	5653	47.0	5620	468
(523–563 K)[a]	497	6692	55.6	15633	1303
(563–613 K)[b]	532	7080	58.9	12811	1068
(613–653 K)[a]	575	7296	60.7	5963	497
(693–773 K)[b]	645	8106	67.4	5537	461
(673–773 K)[a]	670	8262	68.7	3765	314

[a] Measured on CBV-2314.
[b] Measured on 2.5% MnCBV-2314.

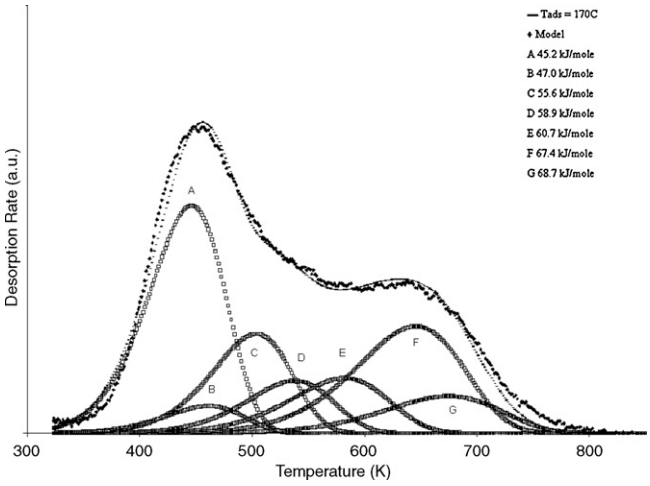

Fig. 4. Typical deconvolution result.

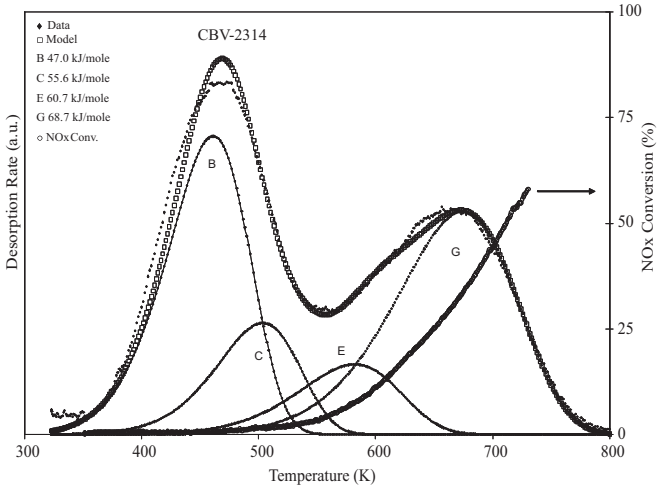

Fig. 6. Comparison of NH_3-SCR activity with NH_3-TPD behaviour of CBV-2314 (0%Mn).

incorporation is immediately seen, as the 0.5%MnCBV-2314 and 1.6%MnCBV-2314 catalysts show enhanced activity between 500 and 600 K relative to CBV-2314. It is also interesting to note that these catalysts seem to be of lower activity than the CBV-2314 at temperatures exceeding approximately 650 K. Further Mn incorporation leads to a large increase in activity, as evidenced by the 1.9%MnCBV-2314 catalyst. This catalyst shows superior activity at all temperatures compared to samples of lower Mn content, reaching 100% NO_x at approximately 575 K. Above this loading, there is an improvement in activity, but as shown by the remaining curves in Fig. 5, the activity resulting from further increases in Mn loading tends to plateau as the Mn loading approaches 100% charge exchange, (3.5% by mass).

3.3. Acidity–activity correlations

In order to relate the observed activity with the TPD behavior of the catalyst series, NO_x conversion data as a function of temperature was superimposed onto the plots of NH_3-TPD data. Example plots are shown in Figs. 6–9. As shown in Fig. 6, CBV-2314 contains at least four distinct sites that can be identified by TPD. These are labeled as sites B, C, E and G. While site B clearly represents a significant fraction of the total population, it is also apparent that this site is completely depopulated of NH_3 at temperatures greater

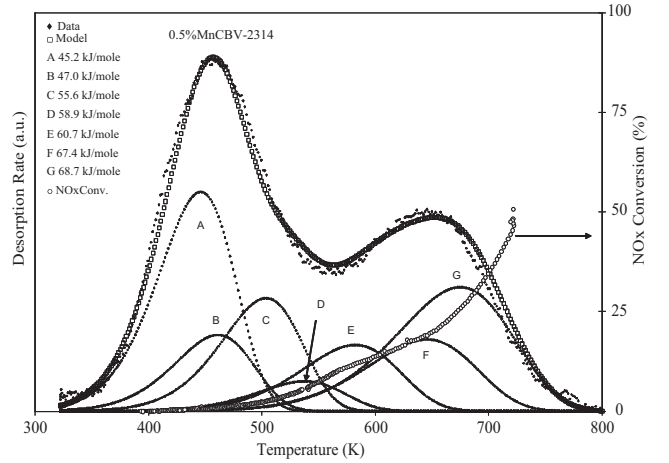

Fig. 7. Comparison of NH_3-SCR activity with NH_3-TPD behaviour of 0.5%MnCBV-2314.

than 550 K under the conditions of our study. The same consideration could be applied to site C, with the result that only sites E and G are significantly populated with NH_3 under the conditions at which non-trivial $DeNO_x$ activity is observed ($T > 550$ K). There-

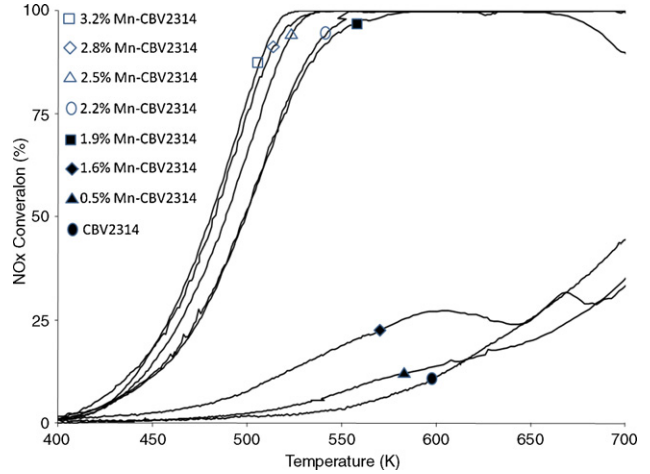

Fig. 5. NH_3-SCR activity of MnCBV-2314 catalysts as a function of temperature for various MnCBV-2314.

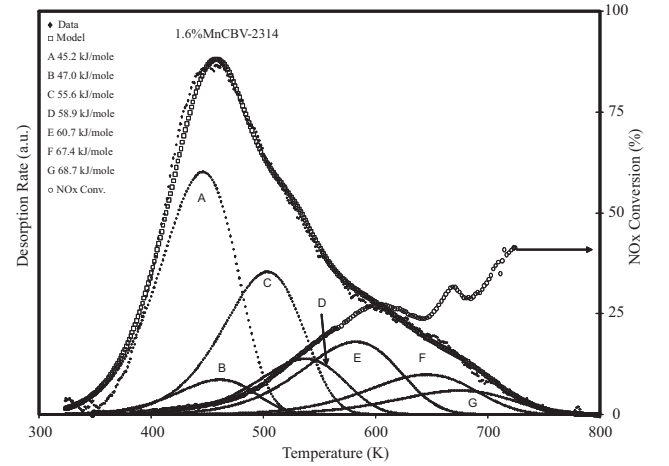

Fig. 8. Comparison of NH_3-SCR activity with NH_3-TPD behaviour of 1.6%MnCBV-2314.

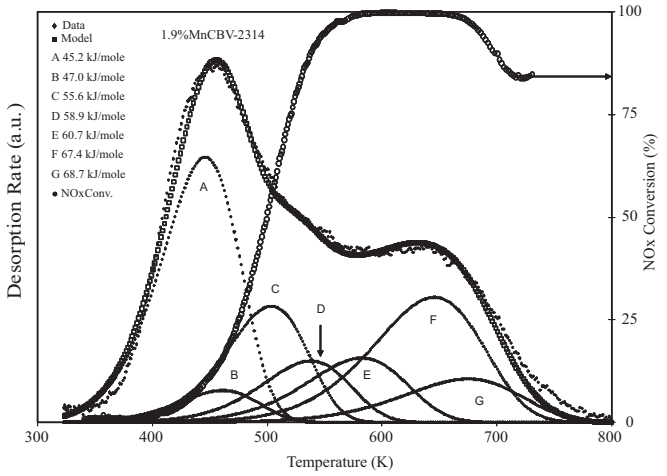

Fig. 9. Comparison of NH_3-SCR activity with NH_3-TPD behaviour of 1.9%MnCBV-2314.

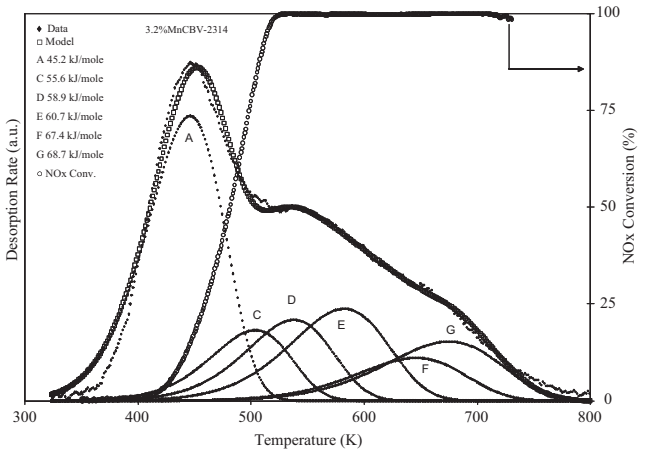

Fig. 10. Comparison of NH_3-SCR activity with NH_3-TPD behaviour of 3.2%MnCBV-2314.

fore only sites E and G are likely to be responsible for the observed activity of CBV-2314.

Referring back to Fig. 5, the 0.5%MnCBV-2314 catalyst exhibits increased $DeNO_x$ activity relative to CBV-2314 at temperatures between 500 and 600 K. In addition to the sites observed in CBV-2314 (B, C, E and G), Fig. 7 shows three novel sites (A, D and F) that can be observed in this catalyst. Sites A and B are not likely responsible for the observed activity of this catalyst, as they are essentially depopulated at temperatures above 500 K. As shown in Figs. 5 and 7, this is also the temperature above which the activity of this catalyst becomes significant. Site C could be excluded based on the analysis of CBV-2314 (above), and site E does not appear to have changed in density, but site D does merit consideration, as do sites F and G. The increased activity (relative to CBV-2314) exhibited by this catalyst at temperatures between 500 and 600 K may be explained by its increased ability to retain NH_3 on its surface under these conditions, as indicated by the densities of sites D and F, especially since these sites were not detected in CBV-2314. Furthermore, as noted previously, this catalyst exhibits lower activity than the CBV-2314 at temperatures exceeding approximately 650 K. Comparing the densities of site G between these catalysts, a lower density is observed in the 0.5%Mn catalyst. This can be explained in terms of the replacement of Brønsted acid sites by Mn ions during the exchange process. Such sites would likely have been formed during high temperature calcination as outlined below [7,18]:

$$NH_4{}^+Z^- \xrightarrow{\Delta T, -NH_3} H^+Z^- \quad (5)$$

This equates to the hypothesis that site G is a Brønsted acid site, whereas at least one or all of the sites A, D and F is a Lewis acid site. By this logic, one could also argue that site B is also a Brønsted site, in that it is replaced by Mn exchange, but further experimentation (such as alkylamine-TPD) would be required to conclusively justify this.

Very similar arguments can made about the behavior of the 1.6%MnCBV-2314 catalyst, which is shown in Fig. 8. Once again the density of site D in noticeably higher compared to samples of lower Mn content, as is the activity at temperatures between 500 K and 600 K. Furthermore, the density of site G is much reduced in this sample, and again this catalyst shows lower activity at elevated temperatures (where site G appears to be responsible for surface NH_3 population) compared to catalysts of lower Mn content.

This trend in activity and acidity continues with the 1.9%Mn catalyst, shown in Fig. 9. Here a further loss in site B with a corresponding increase in site A is observed, again indicating that site B is a likely a Brønsted site, and that site A is likely a Lewis site associated with Mn. Nonetheless, site A (and B, as above) can likely be excluded from consideration in the attempt to explain the activity of this catalyst, as it is significantly depopulated at temperatures above 500 K. Costa et al. [17] applied similar exclusions in their attempts to explain the activity of acidic zeolites. While sites C and E do not change in density, site D and F increase markedly. Based on this, it can be argued that sites C and E may be structural Lewis acid sites [7], such as extra framework alumina species (EFAl) which are not exchanged during the Mn incorporation. It can be further argued that sites D and F are Lewis sites associated with Mn, as their density scales with Mn content. Relative to catalysts of lower Mn content, the increased densities of sites D and F in the 1.9%Mn catalyst, which collectively maintain NH_3 population on the surface of this catalyst at temperatures between 500 and 700 K, correlate with an increased activity of this catalyst at these temperatures. Finally, a further reduction in the density of site G is noted upon further Mn incorporation, thus supporting the hypothesis that site G is a Brønsted site. Also to be noted is that the 1.9%Mn catalyst begins to show decreasing activity at high temperature (ca. 700 K) and this supports the view that site G is at least partially responsible for high temperature activity. Indeed Figs. 5 and 9 suggest that losses in density of site G result in loss of activity at high temperature for the 0.5%, 1.6% and 1.9%Mn catalysts.

Finally, as shown in Fig. 10, the 3.2%Mn catalyst has an increased density of site A, is completely free of site B, and shows very significant $DeNO_x$ activity. This supports the statement that site A and B are likely Lewis and Brønsted sites, respectively, but that these sites are not responsible for the observed activity of the catalyst series. Site C appears not to have changed in density, while the densities of sites D and E have increased only to a small degree. Finally, the density of site F has actually decreased while that of site G has increased. A modest increase in activity is observed at temperatures less than 600 K, and no significant losses at high temperature are observed. This may strengthen the argument that site G retains surface NH_3 necessary for activity at high temperature.

These findings are summarized in Figs. 11–13, which show the densities of each of the acid sites as a function of Mn loading. The general findings are that sites C and E do not vary significantly across the exchange process, and that they are likely structural Lewis sites. Sites A, D and F increase with Mn exchange, and as such are likely Lewis sites resulting from divalent Mn ions or MnO_x type species. While site A was excluded from consideration in the attempt to explain the correlation between activity and acidity, sites D and F appear to correlate well. Not only do the densities of these sites increase as observed activity increases, but their densities also appear to plateau in much the same manner as the activity

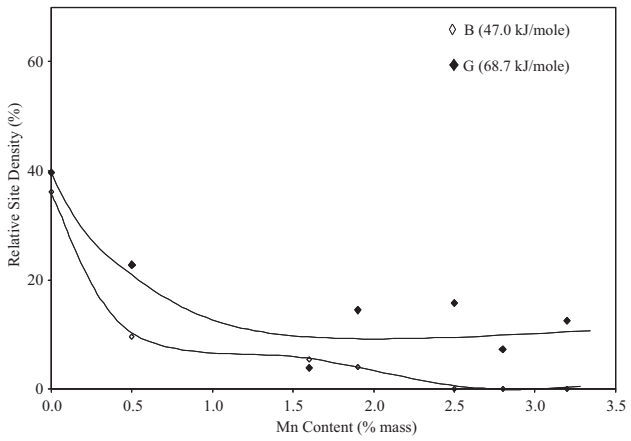

Fig. 11. Variations in density of sites B and G as a function of Mn exchange.

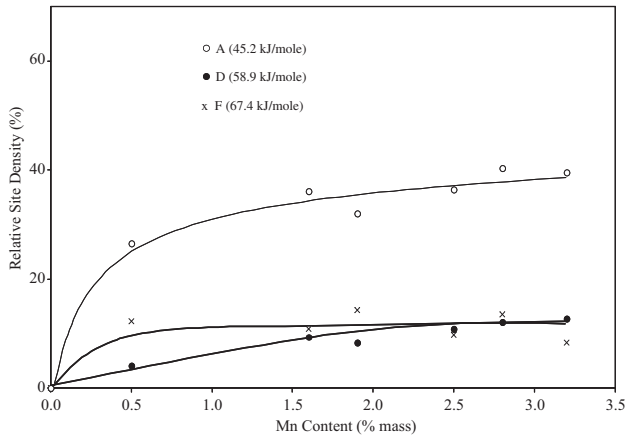

Fig. 12. Variations in density of sites A, D and F as a function of Mn exchange.

reaches a plateau with increasing Mn content. Finally, the densities of site B and G are decreased during the Mn ion-exchange, leading to the conclusion that they are likely Brønsted sites in the CBV-2314.

It is well-known that heating rates affect peak temperatures in TPD experiments according to the following equation [16]:

$$\frac{d\ln(T_P^2/\beta)}{d(1/T_P)} = -\frac{E}{R} \quad (6)$$

The ramp rate employed in the TPD studies was 5 K/min, while the heating rate used in the activity studies varied from 1 K/min

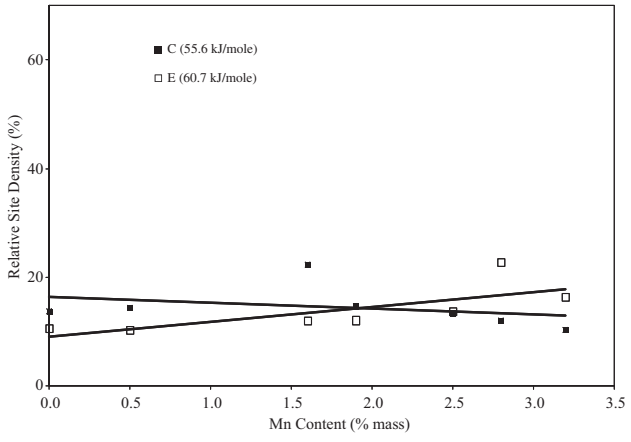

Fig. 13. Variations in density of sites C and E as a function of Mn exchange.

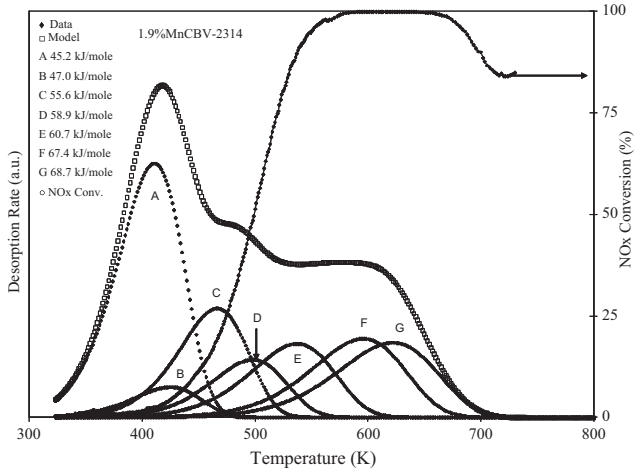

Fig. 14. Recalculation of acid site deconvolution of 1.9%MnCBV-2314 for β = 1.5 K/min.

(350–573 K) to 2 K/min (573–723 K). In order to estimate the effect this difference might have had on the correlation, the acid site deconvolution of the 1.9%MnCBV-2314 catalyst was recalculated for a change in β from 5 K/min to a value of 1.5 K/min (representing the average heating value used during the activity studies). This was accomplished by calculating new T_p values from the known values of E_A. As shown in Fig. 14, the peak temperatures shift to the left by varying amounts (according to varying values of E_A). The correlation that has been drawn between the density of sites which are responsible for increased surface NH_3 population (sites D, F and G) at temperatures where favorable activity is observed (500 K < T < 700 K) is still very much evident. However, the explanation of variations in activity at high temperature appears to be less obvious. When the TPD data is corrected for ramp rate, as in Fig. 14, the sites which may explain high temperature activity appear to be outside the scope of the TPD study. What this means is that the set of basis energies used in the deconvolution procedure cannot be used for extrapolation. Therefore, when the acid site distribution was recalculated at higher ramp rates, (Fig. 14), the model has no means of describing the acidity near 700 K. This is because the acid sites which desorb near 700 K under the higher ramp rate desorb at even higher temperatures at the lower ramp rate, and therefore were not modeled in the study. In order to gain insight into any correlation between activity and acidity at such high temperatures, TPD studies at temperatures exceeding the reaction temperature of interest will be necessary, as discussed in the introductory section of this paper and depicted in Fig. 3. In addition, correlations between acidity and activity at high temperature are further complicated by additional reactions such as NH_3 oxidation.

4. Conclusions

In this report we have demonstrated the correlation between the NH_3-SCR activity of Mn exchanged zeolites and the acidity of such catalysts. Above a threshold of Mn content between 1.6% and 1.9% (by mass), the NH_3-SCR activity of MnCBV-2314 catalysts appears to significantly increase. Further increases in the Mn content towards 100% exchange capacity (3.5% by mass) leads to a plateau in activity of these catalysts. While some of the acid sites detected in this study do not appear correlated with NH_3-SCR activity, increasing the degree of Mn exchange leads to increasing densities of acid sites with NH_3 retention capacity at similar temperatures at which novel activity is observed for T > 500 K. These sites, referred to herein as sites D and F, appear to be Lewis sites, while site G, which retains NH_3 at higher temperatures and shows

a decreasing density with increasing degree of Mn exchange, is considered to be a Brønsted sites. Further experiments, such as alklyamine-TPD, will be required to verify this conclusion. Finally, the explanation of NH_3-SCR activity at higher temperatures than 600 K was outside the scope of the NH_3-TPD studies employed herein.

Acknowledgements

The authors gratefully acknowledge support for this project from Natural Sciences and Engineering Research Council of Canada (NSERC) through the Visiting Fellowships in Government Laboratories program. Also, the authors acknowledge funding provided by Natural Resources Canada through the Program of Energy Research and Development under its Advanced Fuels and Transportation Emissions Reduction (AFTER) program.

References

[1] S. Roy, M. Hegde, G. Madras, Appl. Energy 86 (2009) 2283–2297.
[2] http://www.dieselnet.com/standards/us/ld_t2.php.
[3] M. Yao, Z. Zheng, H. Liu, Prog. Energy Combust. Sci. 35 (2009) 398–437.
[4] M. Zheng, G. Reader, J. Hawley, Energy Convers. Manage. 45 (2004) 883–900.
[5] J. Kelly, M. Stanciulescu, J.-P. Charland, Fuel 85 (2006) 1772–1780.
[6] S. Brandenberger, O. Kröcher, A. Tissler, R. Althoff, Catal. Rev. 50 (2008) 492–531.
[7] J. Weitkamp, Solid State Ionics 131 (2000) 175–188.
[8] L.N. Shil, S. Bhatia, Ind. Eng. Chem. Prod. Res. Dev. 25 (1986) 530–537.
[9] M. Santikunaporn, J.E. Herrera, S. Jongpatiwut, D.E. Resasco, W.E. Alvarez, E.L. Sughrue, J. Catal. 228 (2004) 100–113.
[10] R. Cid, F. Orellana, A. López Agudo, Appl. Catal. 32 (1987) 327–336.
[11] E.J.M. Hensen, J.A.R. van Veen, Catal. Today 86 (2003) 87–109.
[12] S. Putluru, A. Riisager, R. Fehrmann, Appl. Catal. B: Environ. 97 (2010) 333–339.
[13] C. Costa, J.M. Lopes, F. Lemos, F. Ramôa Ribeiro, J. Mol. Catal. A: Chem. 144 (1999) 221–231.
[14] H.W. Nesbitt, D. Banerjee, Am. Miner. 83 (1998) 305–315.
[15] H. Pan, Q. Su, J. Chen, Q. Ye, Y. Liu, Y. Shi, Environ. Sci. Technol. 43 (2009) 9348–9353.
[16] B.R. Greenhalgh, S.M. Kuznicki, A.E. Nelson, Appl. Catal. A: Gen. 327 (2007) 189–196.
[17] C. Costa, I.P. Dzikh, J.M. Lopes, F. Lemos, F. Ramôa Ribeiro, J. Mol. Catal. A: Chem. 154 (2000) 193–201.
[18] N.V. Turutina, O.A. Pilyankevich, A.I. Prilipko, G.M. Tel'biz, V.G. Il'in, Theor. Exp. Chem. 31 (1995) 44–47.